The effect of hydrate content on seismic attenuation: A case study for Mallik 2L-38 well data, Mackenzie delta, Canada

Shyam Chand and Tim A. Minshull

School of Ocean and Earth Science, Southampton Oceanography Centre, Southampton, UK

Received 19 April 2004; revised 8 June 2004; accepted 22 June 2004; published 27 July 2004.

[1] Observations of velocities in sediments containing gas hydrates show that the strength of sediments increases with hydrate saturation. Hence it is expected that the attenuation of these sediments will decrease with increasing hydrate saturation. However, sonic log measurements in the Mallik 2L-38 well and cross hole tomography measurements in the Mallik field have shown that attenuation increases with hydrate saturation. We studied a range of mechanisms by which increasing hydrate saturation could cause increased attenuation. We found that a difference in permeability between the host sediment and the newly formed hydrate can produce the observed effect. We modelled attenuation in terms of Biot and squirt flow mechanisms in composite media. We have used our model to predict observed attenuations in the Mallik 2L-38 well, Mackenzie Delta, Canada. *INDEX TERMS:* 0935 Exploration Geophysics: Seismic methods (3025); 3210 Mathematical Geophysics: Modeling; 5114 Physical Properties of Rocks: Permeability and porosity; 5144 Physical Properties of Rocks: Wave attenuation; 4275 Oceanography: General: Remote sensing and electromagnetic processes (0689). **Citation:** Chand, S., and T. A. Minshull (2004), The effect of hydrate content on seismic attenuation: A case study for Mallik 2L-38 well data, Mackenzie delta, Canada, *Geophys. Res. Lett.*, *31*, L14609, doi:10.1029/2004GL020292.

1. Introduction

[2] Gas hydrates are observed in sediments of continental margin and permafrost regions. Since they increase the shear strength of the host sediment, they increase slope stability. Sediments containing gas hydrates also form an impermeable layer trapping gas beneath it, which could form a future energy resource. Higher velocities than that of water-filled, normally compacted marine sediments can be attributed often to the presence of gas hydrate [*Chand and Minshull*, 2003]. However, it has been observed that presence of gas hydrate can increase attenuation even though the stiffness of the composite matrix is increased. Here we assess the cause of the increase of attenuation with hydrate saturation through mechanisms of fluid flow. We make use of a dataset that includes measurements of compressional and shear wave velocities (V_p, V_s) and attenuation (here defined as Q_p^{-1} and Q_s^{-1}) and the physical properties and composition of the host sediment. The dataset comprises borehole measurements from sand rich sediments in the Mallik 2L-38 well, Mackenzie Delta area [*Guerin and Goldberg*, 2002].

0094-8276/04/2004GL020292$05.00

2. Attenuation Mechanisms

[3] Proposed mechanisms for attenuation in composite materials include the effects of wetting on grain boundaries [*Johnston et al.*, 1979], macroscopic fluid flow [*Biot*, 1956a, 1956b], inter-crack squirt flow [*Mavko and Nur*, 1975], intra-crack flow [*Mavko and Nur*, 1979], viscous shear relaxation [*Walsh*, 1969], flow between macroscopic regions of total and partial saturation [*White*, 1975], scattering [*McCann*, 1969] and friction [*Walsh*, 1966].

[4] However, most of these mechanisms can be ruled out for the case of seismic attenuation in hydrate-bearing sediments. Frictional attenuation is only important at very high strain ($>10^{-6}$) [*Walsh*, 1966], scattering is important only at wavelengths comparable to the size of the grains [*McCann*, 1969] and viscous fluid effects are important only for fluids of high viscosity [*Walsh*, 1969]. Attenuation is negligible in dry rocks [*Tittmann*, 1977], and is strongly dependent on the degree of fluid saturation in rocks containing a free fluid phase [*Murphy et al.*, 1986]. Attenuation is also strongly dependent on effective pressure [*Winkler and Nur*, 1982], decreasing by at least an order of magnitude between ambient pressure and 40 MPa.

[5] *Biot*'s [1956a, 1956b] comprehensive theory of wave propagation in fluid saturated media considers a two-component medium composed of a compressible fluid, which fills the interstices of a compressible porous frame that has shear stiffness and interconnected void spaces. When the rock frame is deformed by an acoustic wave, shear stresses are generated within the pore fluid. These stresses decay exponentially away from the pore wall with a viscous skin depth that decreases with increasing frequency. Thus, the average overall motion of the fluid may be partially out of phase with the motion of the rock frame and part of the total energy loss will be caused by relative motion between the fluid and frame. Dissipation reaches a peak when the viscous skin depth is comparable to the pore size. At low frequencies the skin depth is much larger than the pore diameter, shear stresses are small and viscous energy dissipation is minimal. At high frequencies the skin depth is very small, creating large shear stresses in a very small volume near the pore wall and again energy dissipation is small. However, at intermediate frequencies where the viscous skin depth is comparable to the pore size, moderate shear stresses exist throughout the pore volume and maximum energy dissipation occurs [*Winkler and Nur*, 1982]. *McCann and McCann* [1985] extended Biot's model to include a realistic distribution of pore sizes and were able to predict the variation of attenuation with frequency for unconsolidated water-saturated sands.

[6] Another attenuation mechanism due to fluid is inter-crack squirt flow which may result in significant attenuation

Table 1. Parameters Used in the Models

Parameter	Value
Quartz bulk modulus	36 GPa [*Carmichael*, 1982]
Quartz shear modulus	45 GPa [*Carmichael*, 1982]
Quartz density	2650 kg/m^3 [*Carmichael*, 1982]
Clay bulk modulus	20.9 GPa [*Mavko et al.*, 1998]
Clay shear modulus	6.85 GPa [*Mavko et al.*, 1998]
Clay density	2580 kg/m^3 [*Mavko et al.*, 1998]
Hydrate bulk modulus	7.7 GPa [*Waite et al.*, 2000]
Hydrate shear modulus	3.2 GPa [*Waite et al.*, 2000]
Hydrate density	910 kg/m^3 [*Waite et al.*, 2000]
Water bulk modulus	2.32 GPa [*Carmichael*, 1982]
Water density	1030 kg/m^3
Viscosity of water	2.04×10^{-3} Pa s
Permeability (sediment)	5×10^{-13} m^2 [*Katsube et al.*, 1999]
Permeability (hydrate)	5×10^{-11} m^2
Porosity (hydrate)	0.29
Frequency (P and S waves)	12000 Hz, 2500 Hz

at seismic to ultrasonic frequencies, for both fully saturated [*Mavko and Nur*, 1975] and partially saturated rocks [*Mavko and Nur*, 1979]. Biot's theory seems to predict values of attenuation which are too low to explain the observations, while a squirt flow model predicts the observed values. In partially saturated rocks, compressional wave attenuation is much larger than in fully saturated rocks. Again here also squirt flow can explain the mechanism [*Mavko and Nur*, 1979]. Every crack is partially saturated with the liquid phase wetting the crack surfaces and accumulating at crack tips or at constrictions along the length of the crack. Compression of cracks causes liquid to flow into regions occupied by gas, resulting in viscous energy losses. Bulk compression causes every crack to compress and contribute to the attenuation. Pure shear deformation however does not affect cracks suitably oriented with respect to the stress axes and so results in less attenuation.

[7] Biot's model and the squirt flow model are inferred to act at different length scales. Hence the influence of fluids on attenuation can be represented by a combined poro-elastic wave equation including both Biot and squirt flow (BISQ) mechanisms. In *Dvorkin and Nur*'s [1993] BISQ model the attenuation is considered to be due to viscous friction losses during the flow of fluid imposed by the passing wave. This mechanism appears to dominate seismic wave scattering even at frequencies as high as 1 MHz. The model assumes that the Biot flow takes place in the direction of wave propagation while squirt flow takes place perpendicular to it. The BISQ model relates the dynamic poro-elastic behaviour of a saturated rock to traditional poro-elastic constants, porosity, permeability, fluid compressibility and viscosity, and the characteristic squirt flow length. Similar models combining Biot flow and squirt flow have been developed by others [*Parra*, 2000]. We use an anisotropic model based on constitutive relations, i.e., the total stress tensor of the anisotropic porous medium and the stress tensor in the pore fluid, the momentum balance equation for total stress, and the generalized Darcy's law in the framework of Biot's theory [*Parra*, 2000].

3. Attenuation Model

[8] We use an approach based on the self consistent approximation (SCA) and differential effective medium theory (DEM) [*Jakobsen et al.*, 2000] to relate the seismic properties of hydrate-bearing sediments to their porosity, mineralogy, micro-structure, clay particle anisotropy and hydrate saturation. The initial SCA medium is created using clay and hydrate assuming hydrate is cementing the medium thus increasing the strength of the composite from low gas hydrate saturation [*Chand et al.*, 2004]. We extend this model to include the attenuation effects by including the effects of fluid flow through sediment and hydrate on wave velocities and amplitudes. The amount of attenuation due to fluid flow through the sediment microstructure as well as the hydrate matrix is separately estimated using a poro-elastic model [*Parra*, 2000]. The dry hydrate-bearing sediment modulii are derived using Gassman's equation.

[9] The solutions for the poro-elastic equation [*Parra*, 2000] in terms attenuations are given by

$$Q_p^{-1} = \frac{2imag(k_p)}{real(k_p)}, \quad Q_s^{-1} = \frac{2imag(k_s)}{real(k_s)}, \text{ where}$$

$$k_p = 0.5\left\{ \left(k_{at}^2 + k_{bt}^2 + k_{ct}^2\right) + \sqrt{\left(k_{at}^2 + k_{bt}^2 + k_{ct}^2\right)^2 - 4k_{at}^2 k_{ct}^2} \right\},$$

$$k_s = k_s(s_m) + H * k_s(h_m)$$

$$k_{at} = k_a(s_m) + H * k_a(h_m), \quad k_{bt} = k_b(s_m) + H * k_b(h_m),$$

$$k_{ct} = k_c(s_m) + H * k_c(h_m)$$

$$k_a^2 = {}^{\omega^2 \rho_0}\Big/_{(\lambda + 2\mu)}, \; k_b^2 = {}^{-\alpha_0^2}\Big/_{(\theta(\lambda + 2\mu))}, \; k_c^2 = {}^{-\beta}\Big/_{(\theta)}, \; k_s = {}^{\omega^2 \rho_0}\Big/_{\mu}$$

$$\rho_0 = \rho + \rho_f^2 \omega^2 \theta, \quad \alpha_0 = \alpha + \rho_f \omega^2 \theta,$$

$$\theta = -\left[\frac{j\phi}{\omega \rho_f} \left[\frac{\rho_a/\rho_f + \phi}{\phi} + \frac{j\omega_l}{\omega} \right]^{-1} \Big/ j\omega \right],$$

$$\alpha = 1 - (3\lambda + 2\mu)/3K_s,$$

$$\beta = \phi/K_f + (1-\phi)/K_s - (8\lambda + 5\mu)/9K_s^2, \quad \rho_a = \phi \rho_f (1 - \alpha_l),$$

$$\alpha_l = 1 - r(1 - 1/\phi),$$

$$s = 1 - \frac{2J_1(\gamma R)}{\gamma R J_0(\gamma R)}, \quad \gamma^2 = \frac{\rho_f \omega^2}{(\phi/\beta)} \left[\frac{\rho_a/\rho_f + \phi}{\phi} + \frac{j\omega_l}{\omega} \right],$$

$$\omega_l/\omega = (\eta\phi)/\left(\kappa \rho_f \omega\right)$$

where, the s_m and h_m is the type of matrix, sediment and hydrate respectively, H is percentage of hydrate saturation, r is 0.5 for spheres and changes with grain aspect ratio, ρ_f is the fluid density, R is the squirt flow length, ω is the angular frequency, κ is the intrinsic permeability, ϕ is the porosity, β represents the compressibility coefficient of the undrained hydrate-bearing sediment matrix, J_0 and J_1 are the complex Bessel functions of zero and first order of the first kind, λ and μ are Lame's coefficients of the drained hydrate-bearing sediment and hydrate matrix, K_s and K_f are the bulk modulus of the grain and fluid. The grain moduli are calculated using the Hill's average of the individual grain moduli. Sediment and hydrate have different microstructures, as occurs when there is ice in the pore space [*Durham et al.*, 2003]. The hydrate itself is highly porous with porosity ranging from 0.29 to as much as 0.84 [*Durham et al.*, 2003; *Kelkar et al.*, 1998]. Physical constants used are given in Table 1.

[10] The model predicts that both P and S wave attenuations increase with hydrate saturation. For hydrate saturations above 15–20%, attenuation also increases with frequency until it reaches a peak which is related to the hydrate permeability and then decreases (Figure 1). The

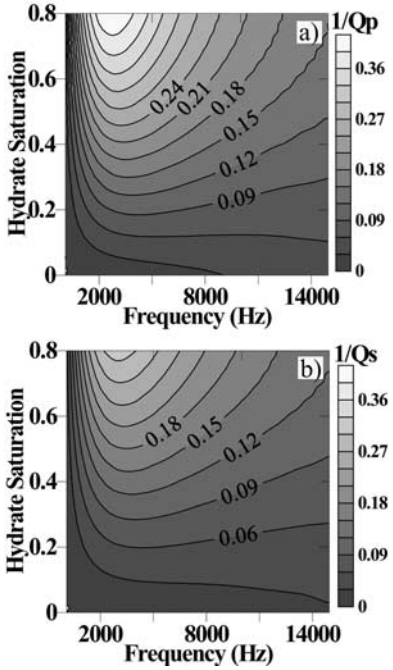

Figure 1. a) P-wave attenuation predicted for sediment with equal amounts of clay and quartz as a function of frequency (Hz) and hydrate saturation (%), b) S wave attenuation predicted for the same sediment.

frequency at which attenuation peaks depends very much on the competing effects of the medium being strengthened by hydrate saturation while the attenuation increases due to a higher proportion of fluid flow in the hydrate matrix.

4. Application to Mallik 2L-38 Well Data

[11] The Mallik 2L-38 well was drilled in a permafrost area with permafrost thickness of 640 metres in the Mackenzie Delta area of Canada [*Collett et al.*, 1999]. NMR spectroscopy as well as Raman spectroscopy and gas to water ratios from a dissociation test showed that the hydrate in the well has properties similar to those of Structure I hydrates [*Uchida et al.*, 1999]. Archie's law interpretation of resistivity logs suggests that gas hydrate occupies an average of 47% of the void space increasing locally to 80% (Figure 2b) [*Winters et al.*, 1999]. Pore waters from the gas-hydrate-bearing samples had an average salinity of 8 ppt compared to 34 ppt for non-gas-hydrate-bearing samples, suggesting that up to 80–90% of the pore space in the gas-hydrate-bearing sediment filled with gas hydrate [*Cranston*, 1999]. Borehole seismic data are also consistent with up to 80% hydrate saturation [*Lee and Collett*, 1999; *Chand et al.*, 2004].

[12] Log data from the Mallik well are summarized in Figure 2. The log measurements were made at 12 kHz and 2.5 kHz for compressional and shear waves respectively [*Guerin and Goldberg*, 2002]. Since the clay content was measured directly only at few depths, estimates based on gamma ray data were used [*Katsube et al.*, 1999; *Chand et al.*, 2004]. We used resistivity derived hydrate saturations, compressional and shear wave velocities and other physical parameters to predict the attenuation using our model. The predicted attenuations are comparable to the observations

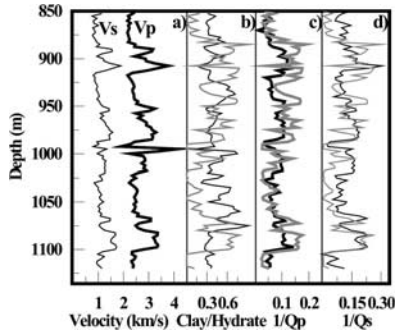

Figure 2. Data from Mallik 2L-38 well, Mackenzie Delta, Canada used in the present study. a) V_p and V_s data from acoustic log measurements [*Collett et al.*, 1999] b) clay content (black line) [*Chand et al.*, 2004] and hydrate saturation (grey line) [*Winters et al.*, 1999] c) Compressional wave attenuation (Q_p^{-1}) observed (black line) and calculated (grey line) (root mean square (RMS) misfit is 13%) d) Shear wave attenuation (Q_s^{-1}) observed (black line) and calculated (grey line) (RMS misfit is 11%) [*Guerin and Goldberg*, 2002]. (The data are smoothed and sampled at 5 m intervals).

(Figures 2c, 2d, and 3). Errors in the predicted values may be attributed to errors in the hydrate saturation inferred from resistivity and to a lesser extent to unmodelled changes in sediment matrix attenuation.

5. Discussion

[13] Attenuation is primarily due to fluid flow within formations. The mechanisms due to fluid flow include the viscous and inertial flow in the direction of wave propagation and perpendicular to it. We observed that, when hydrate forms as a framework within the sediment framework, it has its own fluid flow properties that are different from those in the sediment matrix. Our modelling predicts an increase in attenuation with hydrate saturation and frequency. But the frequency dependent variation depends on the competing factors of sediment strengthening due to hydrate formation

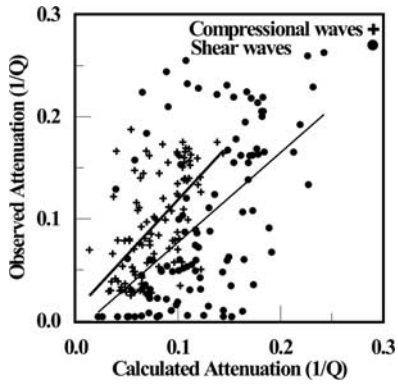

Figure 3. Observed attenuation versus predicted attenuation using resistivity derived hydrate saturation and compressional and shear wave velocities for Mallik 2L-38 well dataset for compressional (plus sign) and shear (dot sign) wave attenuations. Regression fits for both Q_p^{-1} (thick line) and Q_s^{-1} (thin line) are also shown.

and increase of attenuation due to increased fluid flow in the hydrate pore space. The peculiar pattern predicted is justified by observations at a range of frequencies [*Pratt et al.*, 2003; *Guerin and Goldberg*, 2002]. The compressional wave attenuation estimated from cross hole tomography data is observed to increase with hydrate saturation to a maximum of 0.2 with 150–500 Hz in the Mallik field [*Pratt et al.*, 2003] in zones where similar attenuation is measured at 12000 Hz [*Guerin and Goldberg*, 2002]. This similarity can be explained to be due to the fact that these frequencies lie on either side of the peak attenuation frequency band (Figure 1a). Using bore hole data from Mallik 2L-38 well, we are able to relate this increase in attenuation to hydrate saturation. It is also clear that the major influence on attenuation at frequencies above ~200 Hz comes from hydrate, and hence any change in attenuation within hydrate stability zone can be directly related to variations in gas hydrate saturation.

6. Conclusions

[14] From our modelling study, we can draw the following conclusions:

[15] 1. Most of the available mechanisms for attenuation in composite media predict decreasing attenuation with increasing bulk and shear moduli. Hence, in the case of hydrate-bearing sediments, attenuation is expected to decrease as hydrate content increases.

[16] 2. Borehole sonic log data from the Mallik 2L-38 well and cross hole tomographic data from the Mallik field indicate the opposite effect.

[17] 3. These unexpected observations may be explained by an energy loss mechanism involving fluid flow through pores that are within the hydrate matrix.

[18] **Acknowledgments.** This work was funded by the European Union through the HYDRATECH project (EVK3-2000-22060). We thank Dr Gilles Guerin for providing the attenuation data for Mallik 2L-38 well. We also thank Dr. Klaus Bauer and an anonymous reviewer for their constructive comments.

References

Biot, M. A. (1956a), Theory of propagation of elastic waves in a fluid saturated, porous solid. I. Low-frequency range, *J. Acoust. Soc. Am.*, *28*, 168–178.

Biot, M. A. (1956b), Theory of propagation of elastic waves in a fluid saturated porous solid. II. High frequency range, *J. Acoust. Soc. Am.*, *28*, 179–191.

Carmichael, R. S. (1982), *Practical Handbook of Physical Properties of Rocks*, vol. II, CRC Press, Boca Raton, Fla.

Chand, S., and T. A. Minshull (2003), Seismic constraints on the effects of gas hydrate on sediment physical properties and fluid flow: A review, *Geofluids*, *3*, 1–15.

Chand, S., T. A. Minshull, D. Gei, and J. M. Carcione (2004), Elastic velocity models for gas-hydrate bearing sediments—A comparison, *Geophys. J. Int.*, in press.

Collett, T. S., R. E. Lewis, S. R. Dallimore, M. W. Lee, T. H. Mroz, and T. Uchida (1999), Detailed evaluation of gas hydrate reservoir properties using JAPEX/JNOC/GSC Mallik 2L-38 gas hydrate research well down hole well-log displays, *Bull. Geol. Surv. Can.*, *544*, 295–312.

Cranston, R. E. (1999), Pore-water geochemistry, JAPEX/JNOC/GSC Mallik 2L-38 gas hydrate research well, *Bull. Geol. Surv. Can.*, *544*, 165–175.

Durham, W. B., S. H. Kirby, L. A. Stern, and W. Zhang (2003), The strength and rheology of methane clathrate hydrate, *J. Geophys. Res.*, *108*(B4), 2182, doi:10.1029/2002JB001872.

Dvorkin, J., and A. Nur (1993), Dynamic poro-elasticity: A unified model with the squirt and the Biot mechanisms, *Geophysics*, *58*, 523–533.

Guerin, G., and D. Goldberg (2002), Sonic waveform attenuation in gas hydrate-bearing sediments from the Mallik 2L-38 research well, Mackenzie Delta, Canada, *J. Geophys. Res.*, *107*(B5), 2088, doi:10.1029/2001JB000556.

Jakobsen, M., J. A. Hudson, T. A. Minshull, and S. C. Singh (2000), Elastic properties of hydrate-bearing sediments using effective medium theory, *J. Geophys. Res.*, *105*, 561–577.

Johnston, D. H., M. N. Toksoz, and A. Timur (1979), Attenuation of seismic waves in dry and saturated rocks: 2. Mechanisms, *Geophysics*, *44*, 691–711.

Katsube, T. J., S. R. Dallimore, T. Uchida, K. A. Jenner, T. S. Collett, and S. Connell (1999), Petrophysical environment of sediments hosting gas hydrate, JAPEX/JNOC/GSC Mallik 2L-38 gas hydrate research well, *Bull. Geol. Surv. Can.*, *544*, 109–124.

Kelkar, S. K., M. S. Selim, and E. D. Sloan (1998), Hydrate dissociation rates in pipelines, *Fluid Phase Equilibria*, *150–151*, 371–382.

Lee, M. W., and T. S. Collett (1999), Amount of gas hydrate estimated from compressional and shear wave velocities at the JAPEX/JNOC/GSC Mallik 2L-38 gas hydrate research well, *Bull. Geol. Surv. Can.*, *544*, 313–322.

Mavko, G., and A. Nur (1975), Melt squirt in the asthenosphere, *J. Geophys. Res.*, *80*, 1444–1448.

Mavko, G., and A. Nur (1979), Wave attenuation in partially saturated rocks, *Geophysics*, *44*, 161–178.

Mavko, G. T., T. Mukherji, and J. Dvorkin (1998), *The Rock Physics Handbook–Tools for Seismic Analysis in Porous Media*, Cambridge Univ. Press, New York.

McCann, C. (1969), Compressional wave attenuation in concentrated clay suspensions, *Acustica*, *22*, 352–356.

McCann, W. F., and D. M. McCann (1985), A theory of compressional wave attenuation in non-cohesive sediments, *Geophysics*, *50*, 1311–1317.

Murphy, W. F., K. W. Winkler, and R. L. Kleinberg (1986), Acoustic relaxation in sedimentary rocks: Dependence on grain contacts and fluid saturation, *Geophysics*, *51*, 756–766.

Parra, J. O. (2000), Poro-elastic model to relate seismic wave attenuation and dispersion to permeability anisotropy, *Geophysics*, *65*, 202–210.

Pratt, R. G., K. Bauer, and M. Weber (2003), Crosshole waveform tomography velocity and attenuation images of arctic gas hydrates, paper presented at 73rd annual meeting, Soc. of Explor. Geophys., Dallas, Texas.

Tittmann, B. R. (1977), Lunar rock Q in 3000–5000 range achieved in the laboratory, *Philos. Trans. R. Soc. Am.*, *285*, 475–479.

Uchida, T., R. Matsumoto, A. Waseda, T. Okui, K. Yamada, T. Uchida, S. Okada, and O. Takano (1999), Summary of physico-chemical properties of natural gas hydrate and associated gas-hydrate-bearing sediments, JAPEX/JNOC/GSC Mallik 2L-38 gas hydrate research well, by the Japanese research consortium, *Bull. Geol. Surv. Can.*, *544*, 205–228.

Waite, W. F., M. B. Helgerud, A. Nur, J. C. Pinkston, L. A. Stern, S. H. Kirby, and W. B. Durham (2000), First laboratory measurements of compressional and shear wave speeds through pure methane hydrate, *Ann. N. Y. Acad. Sci.*, *912*, 1003–1010.

Walsh, J. B. (1966), Seismic attenuation in rock due to friction, *J. Geophys. Res.*, *71*, 2591–2599.

Walsh, J. B. (1969), New analysis of attenuation in partially melted rock, *J. Geophys. Res.*, *74*, 4333–4337.

White, J. E. (1975), Computed seismic speeds and attenuation in rocks with partial gas saturation, *Geophysics*, *40*, 224–232.

Winkler, K., and A. Nur (1982), Seismic attenuation: Effects of pore fluids and frictional sliding, *Geophysics*, *47*, 1–15.

Winters, W. J., S. R. Dallimore, T. S. Collett, T. J. Katsube, K. A. Jenner, R. E. Cranston, J. F. Wright, F. M. Nixon, and T. Uchida (1999), Physical properties of sediments from the JAPEX/JNOC/GSC Mallik 2L-38 gas hydrate research well, *Bull. Geol. Surv. Can.*, *544*, 95–100.

S. Chand and T. A. Minshull, School of Ocean and Earth Science, Southampton Oceanography Centre, European Way, Southampton SO14 3ZH, UK. (chand@soc.soton.ac.uk)